The radial distribution function probed by X-ray absorption spectroscopy

1994 J. Phys.: Condens. Matter 6 8415

(http://iopscience.iop.org/0953-8984/6/41/006)

J. Phys.: Condens. Matter 6 (1994) 8415–8427. Printed in the UK

The radial distribution function probed by x-ray absorption spectroscopy

Adriano Filipponi

Dipartimento di Fisica, Università degli Studi dell' Aquila, Via Vetoio, 67010 Coppito, L'Aquila, Italy

Received 16 May 1994, in final form 6 August 1994

Abstract. Structural information on the pair distribution function $g_2(r)$ for single-component disordered systems is usually obtained from the experimental structure factor $S(k)$ measured by diffraction techniques. Complementary short-range information can be provided by the analysis of the extended x-ray absorption fine structure $\chi(k)$ associated with a certain x-ray absorption edge. The intrinsic differences in the nature of the $\chi(k)$ and $S(k)$ signals are discussed and particular effort is devoted to connecting the $\chi(k)$ signal with usual quantities familiar to the distribution function theory in disordered matter. An example of the short-range $\chi(k)$ sensitivity is presented showing signals associated with $g_2(r)$ functions of liquid Cu at 1150 °C and 1300 °C. The necessity to fit realistic $g_2(r)$ models to EXAFS spectra satisfying both long-distance behaviour and the compressibility sum rule is emphasized. A method to combine these constraints and previous information on $g_2(r)$ with available $\chi(k)$ data is proposed and applied to recent EXAFS data on liquid palladium.

1. $S(k)$ and $\chi(k)$

Diffraction techniques [1, 2] are certainly the major source of information to probe and understand pair correlations in disordered solids or liquids [3]. The object of the measurement is the structure factor $S(k)$ defined, for a monatomic system, by

$$S(k) = 1 + \frac{4\pi\rho}{k}\int_0^\infty (g_2(r) - 1)r\sin(kr)\,\mathrm{d}r \tag{1}$$

where ρ is the density of the material, and k is the scattering wavevector modulus $k = 4\pi/\lambda\sin(\theta/2)$. $S(k)$ contains information on the radial distribution function $g_2(r)$ defined by the ratio between the average radial density, at distance r from any single atom, and the average macroscopic density. In the absence of long-range order the spatial correlations decay and the following well known long-range limit holds

$$\lim_{r\to\infty} g_2(r) = 1. \tag{2}$$

The number of atoms contained in a shell is obtained by integrating the function $4\pi\rho r^2 g_2(r)$ in the appropriate distance interval. Several methods are available to invert equation (1) to obtain an experimental determination of the $g_2(r)$. They range from the simple Fourier transformation technique [1], to the full three-dimensional modelling obtained by the reverse Monte Carlo (RMC) method [4].

The structural information contained in the $S(k)$ is complete and includes short-range as well as medium- and long-range information. The latter becomes evident upon

0953-8984/94/418415+13$19.50

crystallization of the specimen with the dramatic modification of the diffraction pattern from diffuse rings to sharp rings.

The interest in understanding disordered systems has long stimulated the development of complementary structural techniques. Among these x-ray absorption spectroscopy (XAS) [5, 6] as acquired a central role due to the atomic selectivity. The structural information is contained in the oscillating behaviour of the absorption cross-section affecting the first few hundreds of eV above any deep-core-level excitation threshold. The so-called extended x-ray absorption fine structure (EXAFS) is defined as the relative variation of the absorption cross-section, with respect to the atomic contribution $\sigma_0^t(E)$, normalized by the atomic cross-section of the selected edge $\sigma_0(E)$, and is given by $\chi(k) = [\sigma(E) - \sigma_0^t(E)]/\sigma_0(E)$, where $k = \sqrt{2m(E - E_0)}/\hbar$ is the modulus of the photoelectron wavevector (E_0 is the threshold energy).

$\chi(k)$ is known to be due to interference effects in the transition matrix element associated with the presence of neighbouring atoms. The theoretical understanding of the EXAFS has been the subject of many advances in the last few years [7], that allow us nowadays to perform a reliable data analysis based on theoretical standards [8].

For a given $g_2(r)$ the associated $\chi(k)$ signal can be calculated in a straightforward manner using the equation

$$\chi(k) = \int_0^\infty 4\pi r^2 \rho \; g_2(r) \; \gamma^{(2)}(r, k) \; \mathrm{d}r \tag{3}$$

where the function $\gamma^{(2)}(r, k)$ is the EXAFS signal associated with the presence of a single atom at distance r from the photoabsorber. $\gamma^{(2)}(r, k)$ represents the kernel of the integral equation relating $g_2(r)$ to $\chi(k)$, and is equivalent to the sine function in equation (1), but, unfortunately, its exact shape depends upon the approximations in the theory. For this reason different expressions have been reported in the literature and this has often generated confusion. In fact there is no agreement yet in the scientific community on the way to write equation (3). This is not only due to the early development stage of the technique, but also reflects substantial differences in the theories. In practice the actual closed form expression for $\gamma^{(2)}(r, k)$ involves the summation over many angular momentum partial waves and the phase shifts for the central and back-scattering atomic potentials. A full account of the most efficient present schemes to calculate the $\gamma^{(2)}(r, k)$ function will be reported elsewhere [9]. The formalism presented in this paper is rather general, adaptable to further theoretical improvements, and directly capable of relating the $\chi(k)$ signal to the quantities familiar to the distribution function theory in disordered matter.

Due to the oscillating character of the EXAFS signal, with a typical frequency in k space twice the distance r of the neighbour, $\gamma^{(2)}(r, k)$ is usually written as

$$\gamma^{(2)}(r, k) = A(k, r) \sin(2kr + \phi(k, r)) \tag{4}$$

where the amplitude and phase functions are now smoother functions of either k and r. Notice that the leading phase term has a $2kr$ dependence whereas the equivalent quantity in equation (1) is kr, for this reason the EXAFS k is approximately equal to twice the diffraction k. In the plane wave approximation the phase function $\phi(k, r)$ is linear in k and does not depend upon r, and for this reason simplified equations are often found, but since spherical wave effects are recognized as important [10] we prefer to use the most general expression (4).

In spite of the infinite apparent upper integration limit in (3) the sensitivity of the $\chi(k)$ oscillations to the surrounding structure is actually limited to the neighbourhood of the photoabsorber atom. This is due to two main limiting factors; the first is a simple r^{-2}

spherical decay of the intensity of the interference effects and the second is the presence of a finite mean free path λ for the photoelectron that generates a further exponential damping term, that eventually dominates. The typical range of the EXAFS structural information is in practice contained within 5–10 Å from the photoabsorber atom. In the present notation the amplitude function actually contains the damping factors that are often written as

$$A(k,r) = \frac{f(k,r)}{kr^2} \exp(-r/\lambda(k,r)). \tag{5}$$

Equation (5) was particularly convenient in the plane wave approximation where $f(k,r) = f(k)$, but since modern theories are more complicated we prefer to use a more general expression. Also the $\lambda(k,r)$ term in the modern schemes, that use a complex potential, is not the simple electron mean free path. It actually comes out as an atom dependent energy and distance dependent function. The action of the exponential term is in any case very important since it actually operates as a convergence factor in the integral of equation (3). This produces a substantial difference between the structural information contained in the $S(k)$ and in the $\chi(k)$ functions. In $\chi(k)$ there is an enormous weight on the shortest interatomic distances occurring in the system, but there is no sensitivity to the $g_2(r)$ long-distance tail. A noticeable experimental consequence of the short-range sensitivity is that the typical XAS spectra hardly change upon melting of the specimen. This is usually true for monatomic systems with a few exceptions. One of these is represented by c-Ge that above the melting temperature becomes a metallic liquid with a dramatic change in the average local arrangement [11].

There are further extremely important conceptual differences between equation (1) and (3). In the latter there is no contribution from the space region between $r = 0$ and $r = r_{\min}$ the shortest interatomic approach distance. This distance range is instead essential in the former to give the appropriate $S(k)$ behaviour. Moreover, there is no equivalent for the $\chi(k)$ of the well known compressibility limit for the $S(k)$ that provides a fundamental sum rule for the $g_2(r)$

$$\lim_{k\to 0} S(k) = 1 + 4\pi\rho \int_0^\infty (g_2(r) - 1)r^2 \, \mathrm{d}r = \frac{\rho k_T}{\beta} \tag{6}$$

where k_T is the isothermal compressibility and $\beta = 1/k_B T$ as usual. The lack of such an equivalent property is certainly one of the main reasons for the difficulty of analysis of the $\chi(k)$ information in disordered system. From all the previous consideration it is clear that the inversion of the structural information in the EXAFS signal is not able to provide the full $g_2(r)$ distribution.

2. Previous EXAFS investigations

EXAFS has been widely used to provide local information on the $g_2(r)$ of disordered systems typically including the coordination numbers, average distances and variances of shells of atoms surrounding the photoabsorber. There have been a large number of papers devoted to the problem of how to handle the configurational average of equation (3) in highly disordered systems. Eisenberger and Brown [12] first pointed out the effects of highly asymmetric peaks occurring in disordered systems. A large number of careful investigations have also been performed on superionic conductors by Boyce and co-workers [13] and methods have been devised to tackle highly disordered systems and possibly asymmetric peak shapes [14]. Several studies dealing with actual spectra of liquid systems [15] have posed the problem in the correct framework equivalent to equation (3).

Many EXAFS investigations on disordered systems assume that the signal is sensitive to the 'first coordination shell' of neighbours only. Under these conditions equation (3) reduces to the configurational average over a broad and usually asymmetric peak. An exact analytical method to account for spherical wave effects in the configurational average has been developed by Brouder [16] and generalized to multiple-scattering contributions [17]. In recent papers the average is often performed in the framework of the cumulant expansion method [18, 14], where amplitude and phases are fitted with even and odd Taylor expansions in $k = 0$ respectively. The difficulties and the limitations of this and connected approaches have been widely discussed [14]. In particular it is found that the lack of low-k data represents a major limitation on the possibility of obtaining reliable peak shapes. We point out that due to the intrinsic differences between equation (3) and (1) discussed above the missing low-k EXAFS data do not necessarily play the same role as the low-k $S(k)$ data. A method has been developed [19] to extrapolate the $\chi(k)$ signal to $k = 0$ based on the cumulant expansion approach. In this way it was possible to apply directly the Fourier inversion algorithm to the EXAFS data providing a model free determination of the $g_2(r)$. Again, the intrinsic limitations of the method were clearly stated [19] and the reported applications were limited to disordered crystal examples with a very little insight on the real $g_2(r)$ determination problem.

A general problem that has certainly to be clarified is how to compare first-shell peak information provided by EXAFS with complete $g_2(r)$ functions derived from $S(k)$ data. In a paper dealing with EXAFS measurements of solid and liquid Pb [20], it has been found that the EXAFS coordination actually drops by a factor of 0.5 upon melting. This occurrence is clearly in contrast with diffraction results [21] where liquid Pb is found to have a simple liquid behaviour with a close packing arrangement associated with typical coordination numbers in the range 10–13 that should be quite comparable with the local structure in a high-temperature FCC solid. The explanation provided by the authors [20] was that it is the atomic diffusion present in the liquid structure that hampers a large number of neighbours from contributing to the EXAFS signal. In our opinion these results and considerations can be misleading. In any case $\chi(k)$ probes the instantaneous position of the surrounding atoms and the actual experiment on a multiatomic sample depends on average equal-time properties and is perfectly described by equation (3).

For the benefit of the scientific debate and the cross-fertilization between different research fields involved in studies of disordered matter, a clarification of the actual sensitivity of EXAFS to $g_2(r)$ is certainly required. The main purpose of the present report is indeed to provide such an insight on the basis of simulations and examples.

3. Short-range sensitivity of $\chi(k)$

The system that has been chosen as an example is liquid copper. Radial distribution functions of l-Cu have been obtained by either neutron [22] or x-ray diffraction [23] and the tabulated $g_2(r)$ functions [21] will be used for the present purpose. In order to simulate the signal that an hypothetical EXAFS experiment would detect we calculated the $\gamma^{(2)}(k, r)$ function for Cu–Cu and performed the integral in equation (3). For the reader's convenience the kernel $\gamma^{(2)}(k, r)$ for discrete values of r, from 2.0 Å to 4.5 Å in steps of 0.1 Å, is reported as a function of k in figure 1. The short-range nature of the $\gamma^{(2)}(k, r)$ function is evident. In the discretized integral calculation each $\gamma^{(2)}(k, r)$ function has been multiplied by the number of atoms associated with the corresponding element $dN = 4\pi\rho r^2 g_2(r)\, dr$. After multiplication by dN it is found that the intensity remains quite high even at the distance of 8 Å from the origin atom. But, as a result of the configurational average almost any

high-frequency contribution is washed out and the average signal substantially resembles a damped version of a low-distance shell. Some care has to be taken to perform numerically the integral (3). In fact while the short-range nature of the kernel certainly allows us to enforce a maximum distance cut-off, this should be smooth to avoid termination ripples. We found it efficient to truncate the integral with half Gaussian window starting in the range 6–10 Å with a standard deviation of 0.5–1.0 Å.

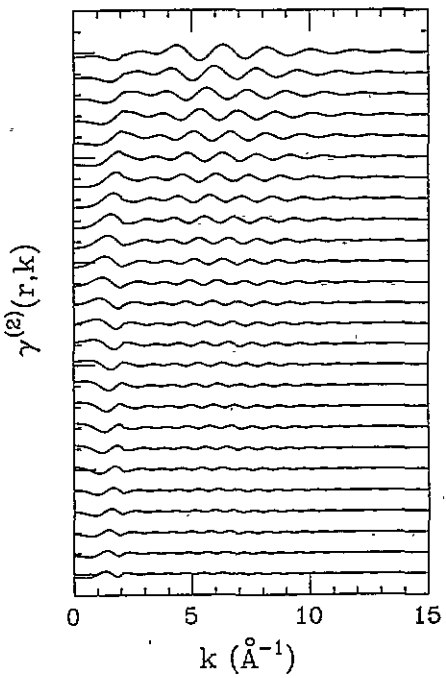

Figure 1. EXAFS kernel $\gamma^{(2)}(k,r)$ calculated for various values of r from 2.0 Å to 4.5 Å in steps of 0.1 Å, as a function of k, for the Cu–Cu pair. The curves are displaced by 0.05 units along the ordinate axis. Notice the short-range nature of the function.

In order to ascertain the sensitivity of the EXAFS signal to possible differences in the $g_2(r)$ we used the available $g_2(r)$ data at two different temperatures and calculated the corresponding $\chi(k)$ signals. These results are shown in figure 2. Panel (a) contains the two model $g_2(r)$ functions used in the present simulations; they refer to liquid copper at 1150 °C (solid curve) and at 1300 °C (dashed curve) [21] respectively. In panel (b) the corresponding $S(k)$, obtained by integrating $g_2(r)$ according to equation (1), are shown. We notice that the slight sharpening of the first-shell peak produces weak effects on $S(k)$, as expected. The effect on the EXAFS signal, shown as $k\chi(k)$ in panel (c) is however much stronger. The main oscillation around $k \approx 5$ Å^{-1} is reduced by nearly 50% for the predicted higher-temperature spectrum. This comparison epitomizes the short-range sensitivity of the EXAFS technique. Finally panel (d) shows the effects of a typical Fourier transformation (FT) of the simulated EXAFS data which is usually applied to judge at a qualitative level the frequency content of the spectra. The magnitudes of the FT data ($F(r)$) show a relatively narrow frequency contribution centred about the short-distance cut-off of the $g_2(r)$ distribution $r \approx 2$ Å. In practice the resulting averaged $\chi(k)$ signal resembles a damped version of a low-distance shell contribution.

The presentation of this simple example clearly shows the complementarity between

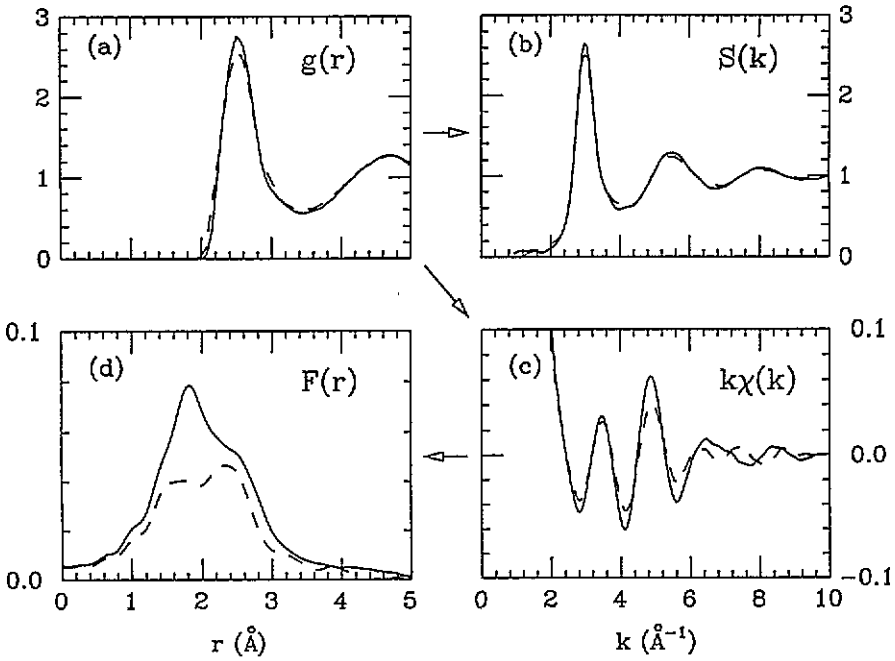

Figure 2. Example of the short-range sensitivity of the EXAFS signal: (a) $g_2(r)$ functions for l-Cu at 1150 °C (solid line) and 1300 °C (dashed line), tabulations derived from an x-ray diffraction experiment [21] (b) corresponding $S(k)$ functions, (c) corresponding $k\chi(k)$ spectra, (d) magnitude of the Fourier transform ($F(r)$) of the $k\chi(k)$ data. Notice that the EXAFS signal is strongly sensitive to slight differences in the first $g_2(r)$ peak whereas the $S(k)$ functions are almost indistinguishable. Notice also that the frequency content of the $k\chi(k)$ spectra corresponds to the first rise of the first peak of $g_2(r)$.

$\chi(k)$ and $S(k)$ data. The $\chi(k)$ contains unique information on the short-range order and might be used to define precisely the shape of the rise of the first $g_2(r)$ peak in a disordered system. If the comparison of figure 2 were done between two $g_2(r)$ data differing, let us say, in the region $r > 5$ Å no difference in the $\chi(k)$ signal would have probably been detected, while $S(k)$ would have been largely modified. In fact, beyond a certain distance, as apparent from equation (5), the $\chi(k)$ is not even sensitive to the presence of the atoms. For this reason the EXAFS data analysis is often limited to the first-shell data only, and longer-distance contributions are actually neglected.

If our aim is the derivation of the $g_2(r)$ of an unknown system it is clear that while a diffraction experiment alone might provide the answer, the EXAFS is hampered in the task. However, it is also clear that a diffraction experiment might be nicely complemented with an EXAFS experiment on the same system. Vice versa, an EXAFS experiment with some external input on the $g_2(r)$, possibly coming from diffraction data or computer simulations might certainly provide an interesting insight as well. All of these considerations widely stimulate the developments of suitable algorithms that use the combined information from $S(k)$ and $\chi(k)$ data. A substantial step forward along this line of research might be represented by the development of the RMC method [4], that has already been applied to the EXAFS data analysis [24]. Another promising approach can be based on the use of regularized inversion algorithms [25].

4. Combining $\chi(k)$ and $S(k)$ data

A simple and efficient method to combine EXAFS data with external information on $g_2(r)$ was proposed by our group, and has been applied so far to the study of liquid Hg [26], to the hydration shell in aqueous solutions of Br^- and of brominated hydrocarbon molecules [27], and to liquid Ge [11].

This method, which will be described in full detail, is also useful, in our opinion, to clarify the role of the complementarity between $\chi(k)$ and $S(k)$. We recall that any reasonable model for $g_2(r)$ should satisfy the long-range behaviour equation (2) and the compressibility sum rule equation (6). For incompressible systems the latter equation simply states, in the thermodynamic limit, that integrating out the $4\pi\rho r^2 g_2(r)$ function one should obtain exactly the number of atoms predicted by the average density of the system. This sum rule has a slight correction due to the density fluctuations in compressible systems, as is well known. Now even if $g_2(r)$ were completely unknown it is a nonsense to try to fit the EXAFS spectrum of a disordered system with a model $g_2(r)$ which does not obey these constraints. Into this class clearly fall all the attempts to account for a single coordination shell, that unfortunately are quite common in EXAFS. The argument often quoted to support the single-shell model is that the spectrum does not contain enough information to fit more than one shell [28]. Our objection is, in fact, that accounting for the correct limit and the sum rule is not fitting additional parameters, it is just starting from the appropriate baseline that is certainly not $g_2(r) = 0$ as usually assumed.

The EXAFS data analysis that we therefore propose for disordered solids or liquids is to start with a model $g_2^m(r)$. This model can be possibly obtained from simple theoretical arguments, molecular dynamics simulations, Monte Carlo simulations, or $S(k)$ data; what is important is that it is realistic and obeys equation (2) and equation (6). Then the appropriate use of EXAFS data is made refining the model, while keeping (2) and (6) valid. Equation (2) implies that the modification of the model should not extend to infinite range, that is quite natural since EXAFS is not sensitive to the long range. In general the difference $\Delta S(k)$ induced by a difference $\Delta g_2(r) = g_2(r) - g_2^m(r)$ can be expanded in Taylor series about $k = 0$:

$$\Delta S(k) = 4\pi\rho \int_0^\infty r^2 \Delta g_2(r) \frac{\sin(kr)}{kr}\, dr$$
$$\approx 4\pi\rho \int_0^\infty r^2 \Delta g_2(r) \left[1 - \frac{k^2}{2!}\frac{r^2}{3} + \frac{k^4}{4!}\frac{r^4}{5} + \dots\right] dr. \tag{7}$$

The compressibility sum rule thus provides an interesting constraint to the zero-order term of (7), namely $\Delta g_2(r)$ should satisfy

$$4\pi\rho \int_0^\infty r^2 \Delta g_2(r)\, dr = 0. \tag{8}$$

In other words the total refined coordination number must not change in the procedure. Further constraints might be obtained requiring that higher-order terms of the Taylor expansion in $k = 0$ remain constant in the refinement. For instance:

$$\left(\frac{\partial^2 \Delta S(k)}{\partial k^2}\bigg|_{k=0}\right) = 0 \quad \leftrightarrow \quad 4\pi\rho \int_0^\infty r^4 \Delta g_2(r)\, dr = 0. \tag{9}$$

This constraint requires that the second moment about $r = 0$ of the short-range probability distribution of finding atoms at distance r should not change. The application of equation (8) and possibly equation (9) can be accomplished in several ways. A trial short-range

$\Delta g_2(r)$ function, that can assume both positive or negative values satisfying (8) and possibly equation (9), might be refined in the procedure. Another equivalent way, described in the previous applications [26, 27, 11] consists in decomposing the $g_2^m(r)$ into a certain number of short-distance peaks (possibly one or two) plus a tail. In the refinement, involving only the short-distance peaks, their total coordination number is kept fixed. In this way it is also guaranteed that $g_2(r) \geqslant 0$ by constraining each coordination number to be non-negative as well.

As an example, if the refinement involves a single peak described by the four parameters N, coordination number, R, mean position, σ^2, variance and β, skewness, equation (8) requires that $\Delta N = 0$, and equation (9) that $\Delta(R^2+\sigma^2) = 0$, leaving only two independent parameters. In the case of the refinement of two asymmetric peaks with parameters N_1, R_1, σ_1^2, β_1 and N_2, R_2, σ_2^2, β_2, respectively, the constraints are

$$\Delta(N_1 + N_2) = 0 \qquad \Delta\left[N_1(R_1^2 + \sigma_1^2) + N_2(R_2^2 + \sigma_2^2)\right] = 0. \tag{10}$$

The application of this method has proven successful in the EXAFS data analysis of disordered systems, and refined $g_2(r)$ functions could be derived. Clearly the validity of the long-range shape of the $g_2(r)$ is based on the quality of the starting model.

5. Application to liquid Pd

An EXAFS spectrum of liquid palladium (l-Pd) at 1870 K has been recently recorded in the framework of an extensive project to study condensed phases of Pd [29] at high temperature. The measurement was performed at the D44-XAS4 beamline (LURE, Orsay, France) equipped with a Si(311) double-crystal monochromator. The high-temperature measurement were performed using a recently developed technique for x-ray absorption studies [30]. In the present paper the spectrum of liquid Pd is used to provide an effective example of the potential of application of EXAFS, in the framework of the present theory, to investigate simple liquid systems.

Liquid Pd was measured by x-ray diffraction [31] and the measured $S(k)$ and calculated $g_2(r)$ have been tabulated [21]. The tabulated $g_2(r)$ for l-Pd at 1580 °C will be assumed as the starting model $g_2^m(r)$. An example of decomposition of the model into two short-range peaks and a long-distance tail is presented in figure 3. In principle any decomposition is perfectly equivalent, the total $g_2^m(r)$ being the only physical quantity. In practice, however, the short-distance peaks should be modelled by using some distribution for which an analytic expression of the EXAFS damping can be worked out, and the tail should be placed to large enough r values that its signal is negligible. In this case we have used a set of four-parameter gamma like distributions, as described elsewhere [27]. Each model peak is completely defined by the coordination number N, average R, variance σ^2 and skewness β. It should be noted that due to the asymmetry their modal value does not generally coincide with R. The algorithm used to calculate the damping of the signal intrinsically accounts for the spherical wave effects. It differs from the one proposed by Brouder [16] because it is based on numerical calculations of the derivative of amplitude and phases [32, 9] rather than on the analytical approach.

The total EXAFS signal associated with the starting model $g_2^m(r)$ is compared with the experimental data in figure 4. We wish to stress that the EXAFS oscillation is clearly detectable up to $k \approx 10$ Å^{-1} corresponding to about $k \approx 20$ Å^{-1} in the diffraction scale, whereas the x-ray diffraction $S(k)$ data [31] are limited to $k \approx 12$ Å^{-1} only. While the amplitude of the simulated signal has the right magnitude, its phase is clearly in disagreement with experiment. The origin of the k scale has been chosen in agreement with the analysis

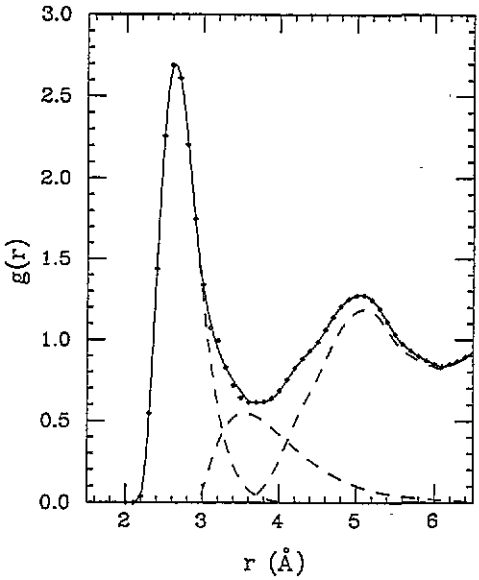

Figure 3. The $g_2(r)$ of l-Pd determined by x-ray diffraction data: decomposition into two short-range peaks and a long-range tail.

of Pd foil spectra (data available from room temperature to just below the Pd melting point) where structural results in agreement with the known Pd–Pd distance have been obtained [33]. In the present context we will not investigate the origin of the discrepancy, it is likely however that it is due to experimental systematic errors in one or possibly both the experiments. We recall that measurements on condensed matter under extreme temperature conditions are in any case extremely difficult.

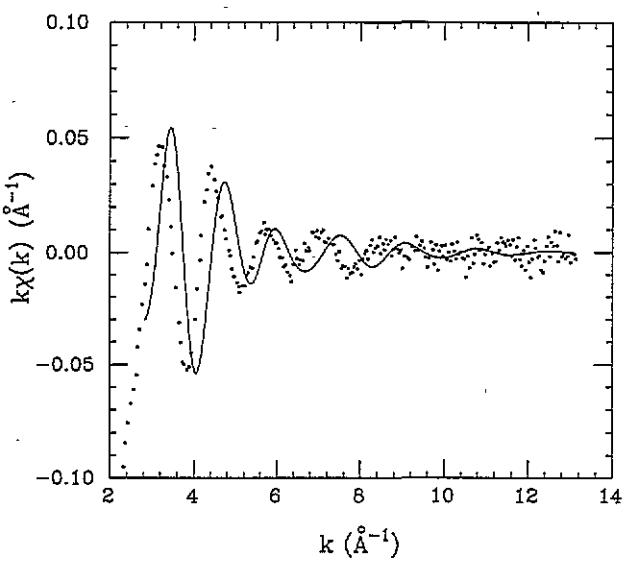

Figure 4. Calculated $k\chi(k)$ signal for the $g_2(r)$ of l-Pd determined by x-ray diffraction (solid line) compared with the EXAFS experiment [29] (dots).

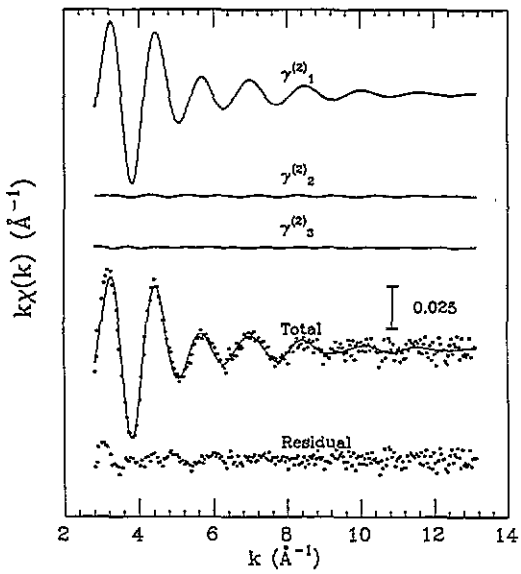

Figure 5. Fitting of the experimental l-Pd EXAFS data. From top to bottom: first peak, second peak and tail contributions, comparison between experimental data (dots) and total model signal (solid curve) and experiment minus model residual difference. The fitting is excellent.

We focus here on the fact that the starting model has to be refined. The refinement is performed following the previously described criteria varying the parameters of the first two peaks but always satisfying the constraints of equation (10). The final results are shown in figure 5. The first three curves from the top represent the contributions from the first peak $\gamma_1^{(2)}$, second peak $\gamma_2^{(2)}$ and tail $\gamma_3^{(2)}$ respectively. The fixed tail signal is in anycase negligible, also the second-peak signal is negligible, but its parameters have been refined in order to accompany the variation of the first-peak parameters which are, however, critical. The successive curves represent the comparison between total model signal (solid line) and the experiment (dots); the agreement is spectacular and the residual (bottom) is dominated by experimental noise only.

The refined model $g_2(r)$ is shown with its three components in figure 6 and it is compared with the starting model. Clearly in order to improve the agreement from figure 4 to figure 5 the first-peak parameters had to be changed. In particular, the phase difference evident in figure 4 required a shift of the first peak by about 0.15 Å in r space. Notice that the maximum of the first $g_2(r)$ peak is now at 2.8 Å whereas that of the initial model was at ≈2.62 Å. Needless to say that this rather large bond length expansion, required to account for the EXAFS oscillation, induces suspicion also of the reliability of the long-range tail of the model that for a close packed liquid is likely to be expanded as well. This possible error, however, does not affect the reliability of the short-range part of the refined $g_2(r)$ shown in figure 6. In fact the EXAFS sensitivity to the short-range structure makes the refined $g_2(r)$ quite reliable up to ≈3.5 Å. In addition the whole model is in any case consistent with the required long-range behaviour and sum rule property any radial distribution function should obey.

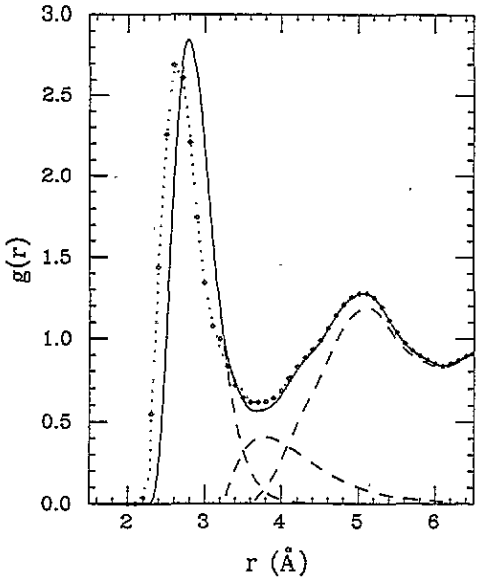

Figure 6. Optimized $g_2(r)$ function for l-Pd that is able to fit the EXAFS data (solid line), compared with the original model (dotted line), the two separate refined peaks and the fixed tail contributions are reported as dashed lines. The optimized $g_2(r)$ is reliable up to about ≈3.5 Å, the range of sensitivity of the EXAFS technique.

6. Conclusions

The results presented in this paper have a certain number of implications for the general understanding of the EXAFS signal in highly disordered systems.

(1) First of all the complementary nature of the structural information contained in $S(k)$ and $\chi(k)$ functions has been widely emphasized with direct examples. In particular the nature of the EXAFS signal has been clarified in terms of quantities familiar to the theory of simple liquids.

(2) Secondly it has been shown that, contrary to what is commonly believed, it is possible to analyse and interpret EXAFS data on liquid systems (or of highly disordered condensed matter in general) in the correct framework of the radial distribution function theory. The erroneous results obtained in the past for liquid Pb [20] are attributed to the failure of the single-shell fitting procedure, even in the version of the cumulant expansion method [18]. Successive developments along this line [19] did not prove capable of deriving radial distribution function information, in spite of the strong claims.

(3) As a third result the importance of refining EXAFS data using realistic $g_2(r)$ models satisfying both long-range asymptotic behaviour and the compressibility sum rule has been stressed, and a practical method to perform this refinement has been proposed. It has been found that the compressibility sum rule can be translated into constraints on coordination numbers and higher even-order moments of the refined short-range atomic probability density $4\pi r^2 \Delta g_2(r)$. These constraints overcome the difficulties present in the single-shell EXAFS fitting due to the correlation between N and σ^2 parameters, from which unphysically low coordination numbers N may result [20]. The proposed method is able to provide reliable $g_2(r)$ shapes in the short range (up to 3.0–4.0 Å), that is, in the region of sensitivity of the EXAFS signal. The reliability of the long-range tail of the refined $g_2(r)$ relies on the

accuracy of the original model.

(4) The method has been applied to a real case of recent EXAFS measurements of liquid Pd, providing a reliable $g_2(r)$ shape up to a distance of $\approx$3.5 Å. In this specific case, it is apparent that the starting model was not correct, in fact a rather large bond length expansion was required to account for the EXAFS oscillation. Although the purpose of this paper was not to discuss the relevance of these findings for the structure of Pd phases at high temperature, it is worth mentioning that the equilibrium crystallographic Pd–Pd distance at room temperature is about 2.75 Å. We estimate, therefore, that it is very unlikely that this distance undergoes a contraction in the liquid phase at 1580 °C as the diffraction data [31] would suggest. The refined $g_2(r)$ on our EXAFS data instead presents a maximum at 2.80 Å that is perfectly compatible with the crystallographic results at room temperature and the expected thermal expansion.

(5) All these findings demonstrate that structural EXAFS investigations of liquid systems under extremely high-temperature conditions might play their own role in the determination of pair correlation properties of even simple liquids. They stimulate further experimental efforts in collecting reliable high-temperature EXAFS data on liquid specimens and point out the strong complementarity between diffraction and EXAFS data. The development of suitable methods able to exploit the combined structural information contained in $S(k)$ and $\chi(k)$ data is also strongly encouraged.

The present report cannot be concluded without warning the reader that the real situation is rather more complex than what is presented here. Indeed the EXAFS signal is not only dependent on the pair correlation properties [9]. There is a further higher-order contribution arising from coherent multiple-scattering effects that makes the $\chi(k)$ also sensitive to triplet and possibly higher-order correlations [34]. The presence of these signals and their importance even in spectra of disordered solids and liquid systems has been widely emphasized by our group [34, 26, 35, 11]. It is exactly this sensitivity to triplet correlations that has stimulated a wide interest in the understanding of the EXAFS signal and its possible applications to derive unique structural information on short-range features of the $g_3(r_1, r_2, \theta)$ distribution. No further progress in this field can however be made without a clear understanding of the pair information contained in the $\chi(k)$ signal which the present contribution has been trying to shed light on.

Acknowledgments

The author is grateful for friendly hospitality among the Neutron Scattering Group at the Physics Laboratory, University of Kent at Canterbury.

References

[1] Warren B E 1969 *X-ray Diffraction* (New York: Dover)
[2] Lovesey S W 1984 *Theory of Neutron Scattering from Condensed Matter* (New York: Oxford University Press)
[3] March N H, Street R A and Tosi M (ed) 1985 *Amorphous Solids and the Liquid State* (New York: Plenum)
[4] McGreevy R L and Pusztai L 1988 *Mol. Simul.* **1** 359
[5] Lee P A, Citrin P, Eisenberger P and Kincaid B 1981 *Rev. Mod. Phys.* **53** 769
Teo B K and Joy D C 1981 *EXAFS Spectroscopy, Techniques and Applications* (New York: Plenum)
Hayes T M and Boyce J B 1982 *Solid State Physics* vol 37, ed H Ehrenreich, F Seitz and D Turnbull (New York: Academic) p 173
[6] Koningsberger D C and Prins R (ed) 1988 *X-ray Absorption* (New York: Wiley)
[7] Chou S-H, Rehr J J, Stern E A and Davidson E R 1987 *Phys. Rev.* B **35** 2604

Dan Lu and Rehr J J 1988 *Phys. Rev.* B **37** 6126
Tyson T A, Hodgson K O, Natoli C R and Benfatto M 1992 *Phys. Rev.* B **46** 5997
[8] Binsted N, Campbell J W, Gurman S J and Stephenson P C 1991 *SERC Daresbury Laboratory EXCURV92 program*
Filipponi A, Di Cicco A, Tyson T A and Natoli C R 1991 *Solid State Commun.* **78** 265
Mustre de Leon J, Rehr J J, Zabinsky S I and Albers R C 1991 *Phys. Rev.* B **44** 4146
Rehr J J, Mustre de Leon J, Zabinsky S I and Albers R C 1991 *J. Am. Chem. Soc.* **113** 5135
[9] Filipponi A, Di Cicco A and Natoli C R 1994 submitted
[10] Gurman S J, Binsted N and Ross I 1984 *J. Phys. C: Solid State Phys.* **17** 143
[11] Filipponi A, Ottaviano L and Di Cicco A 1994 submitted
[12] Eisenberger P and Brown G S 1979 *Solid State Commun.* **29** 481
[13] Boyce J B, Hayes T M and Mikkelsen J C Jr 1980 *Solid State Commun.* **35** 237; 1981 *Phys. Rev.* B **23** 2876
[14] Crozier E D, Rehr J J and Ingalls R 1988 *X-ray Absorption* ed D C Koningsberger and R Prins (New York: Wiley) p 373
[15] Crozier E D and Seary E A 1980 *Can. J. Phys.* **58** 1388
[16] Brouder C 1988 *J. Phys. C: Solid State Phys.* **21** 5075
[17] Brouder C and Goulon J 1989 *Physica* B **158** 351
[18] Bunker G 1983 *Nucl. Instrum. Methods* **207** 437
[19] Stern E A, Ma Y and Hanske-Petitpierre O 1992 *Phys. Rev.* B **46** 687
[20] Stern E A, Livinš P and Zhang Z 1991 *Phys. Rev.* B **43** 8850
[21] Waseda Y 1980 *The Structure of Non-crystalline Material, Liquids and Amorphous Solids* (New York: McGraw-Hill)
[22] Breuil M and Tour and G *J. Phys. Chem. Solids* **31** 549
[23] Waseda Y and Ohtani M 1974 *Phys. Status Solidi* b **62** 535
[24] Gurman S J and McGreevy R L 1990 *J. Phys.: Condens. Matter* **2** 9463
[25] Babanov Y A, Vasin V V, Ageev A L and Ershov N V 1981 *Phys. Status Solidi* b **105** 747
Ershov N V, Ageev A L, Vasin V V and Babanov Y A 1981 *Phys. Status Solidi* b **108** 103
[26] Ottaviano L, Filipponi A, Di Cicco A, Santucci S and Picozzi P 1993 *J. Non-Cryst. Solids* **156–158** 112
[27] D'Angelo P, Di Nola A, Filipponi A, Pavel N V and Roccatano D 1994 *J. Chem. Phys.* **100** 885
[28] Stern E A 1993 *Phys. Rev.* B **48** 9825
[29] Filipponi A and Di Cicco A 1994 unpublished
[30] Filipponi A and Di Cicco A 1994 *Nucl. Instrum. Method Phys. Res.* B **93** 302
[31] Waseda Y and Ohtani M 1975 *Z. Phys.* B **21** 229
[32] Benfatto M, Natoli C R and Filipponi A 1989 *Phys. Rev.* B **40** 9626
[33] Filipponi A and Di Cicco A 1994 submitted
[34] Filipponi A, Di Cicco A, Benfatto M and Natoli C R 1990 *Europhys. Lett.* **13** 319
[35] Di Cicco A and Filipponi A 1993 *J. Non-Cryst. Solids* **156–158** 102; 1994 *Europhys. Lett.* **27** 407